Supporting Information:

Redox-Active Porous Polymer Based on Poly (Imides-Triazine) As High-Performance Cathode for Lithium-ion Batteries

Refka El Oueslati,[a] Badr Jismy,*[a] Benjamin Flamme,[a] Nicolas Leclerc,[b] Fouad Ghamouss*[ac] and Mohamed Abarbri*[a]

List of contents

Table S1. Elemental analysis results of PIT network compared with literature.

X_{eq} of MA	X_{eq} of PMDA	Solvant	T (°C)	Time (h)	Chemical formula	Theoretical values (%)	Found values (%)	Ref
1	1	Without solvent	325	5	--	C : 50.64 N : 27.27 H : 1.30	C : 49.61 N : 29.66 H : 1.54	1
1	1	Without solvent	325	4	$C_{13}H_4N_6O_4$	C : 50.66 N : 27.27 H : 1.31	C : 49.52 N : 28.70 H : 2.20	2
			1011	7 min	$C_{12}H_2N_4O_4$	C: 54.1 N: 21.1 H: 0.8	C: 47.1 N: 26.2 H: 2.4	3
1	1	Without solvent	325	4	--	--	C : 45.49 N : 26.68 H : 2.14	4
1	1	Without solvent	325	4	$C_{12}H_2N_4O_4$	C: 54.1 N: 21.1 H: 0.8	C: 47.9 N: 27.3 H: 2.3	5
1	1.5	Distilled DMSO-Toluene	180	72	$C_{18}H_3N_6O_6$	C : 54.15 N : 21.05 H : 0.76	C : 42.00 N : 40.58 H : 5.15	6
1	1.5	DMSO	180	12				7
1	1.5	Dry DMSO	180	72	$C_{18}H_3N_6O_6$	C : 54.15 N : 21.05 H : 0.76	C : 38.42 N : 33.76 H : 5.42	This Work

Table S2. Specific surface area, and pore volume parameters for the PIT

Synthesis procedure	S_{BET}[a]/m^2 g^{-1}	V_{total}[b]/ cm^3 g^{-1}	V_{micro}[c]/cm^3 g^{-1}	V_{meso}[d]/cm^3 g^{-1}	Ref
Solvothermal	660	0.60	0.21	0.39	6
	430	—	—	—	7
	635.5	0.98	0.04	0.94	8
	674.26	0.543	0.267	0.276	This Work
Solid-state thermal	3.929	—	—	—	1
	1.6	—	—	—	3
	40	—	—	—	9
	7.322	—	—	—	10
	4.39	—	—	—	11

[a] Specific surface area calculated by a Brunauer-Emmett-Teller (BET) method.

[b] Total pore volume determined at $P/P_0=0.99$.

[c] Micropore volume calculated by a Horvath–Kawazoe (HK) method.

[d] Mesopore volume determined by $V_{total} - V_{micro}$.

Table S3. Summary of the literature on different characterization techniques

Synthesis procedure	FT-IR	^{13}C NMR	EA	TGA	SEM	EDS mapping	BET	XRD	XPS	Ref
Solvothermal	M	✓	M	M	I	—	M	M	—	6
	I	—	—	—	—	—	I	M	—	7
	I	—	—	M	I	—	I	—	—	8
	—	—	—	—	—	—	—	✓	—	12
	M	—	M	I	M	—	M	M	—	This Work
Solid-state thermal	I	—	I	I	I	—	I	I	✓	1
	I	✓	I	I	I	—	—	I	—	2
	I	—	I	—	I	✓	I	I	—	3
	I	—	I	—	—	—	—	I	✓	4
	I	—	I	I	I	—	—	I	—	5
	I	—	—	M	—	—	I	I	—	9
	I	—	—	M	I	—	I	I	✓	10
	I	—	—	—	I	—	I	I	✓	11
	I	—	—	—	I	—	—	I	—	13

(—) = not provided or performed. ✓= provided or performed. I= provided but inconsistent. M= provided and matches proposed structure.

Table S4 Performance comparison of our PIT with examples from the literature

Structure	Exp. Capacity/current	Cap. retention/cycles/current	Ref.
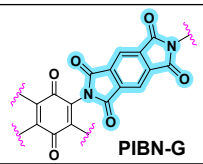 PIBN-G	193.1/10 C (+ rGO)	86% / 300 / 1 C	14
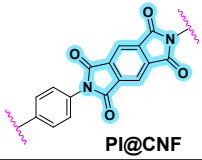 PI@CNF	170/1 C (0.175 A g^{-1}) (+ CNF)	81.3% / 1000 / 1 C (175 mA g^{-1})	15
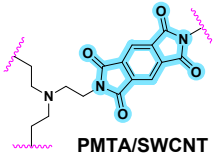 PMTA/SWCNT	160/0.1 C (+ SWCNT)	80%/1000/0.5 C	16
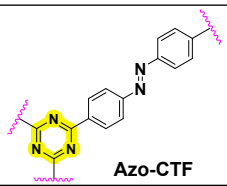 Azo-CTF	205/0.1 A g^{-1}	89.1% / 5000 / 4 A g^{-1}	17

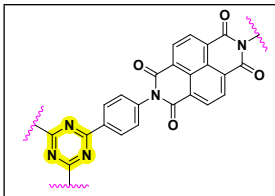 TAPT-NTCDA@CNT	155/0.05 A g^{-1} (+ CNT)	87.3% / 500 / 1 A g^{-1}	18
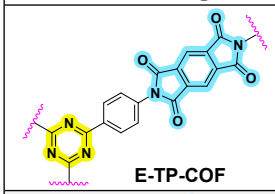 E-TP-COF	30/2 A g^{-1} (exfoliation)	87.3%/500/0.2 A g^{-1}	19
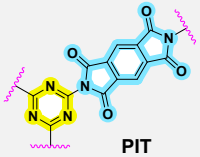 PIT	268/25 C (10 A g^{-1})	65%/4000/15 C (6 A g^{-1})	This Work

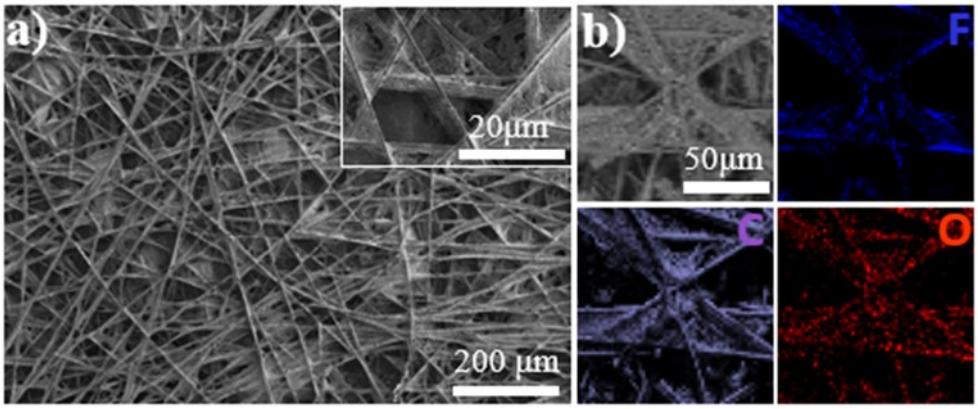

Fig. S1. Microscopic Characterization of the current collector (Sigracet 25 BC) (a) SEM images. (b) EDS elemental mapping images of fluorine, carbon, and oxygen.

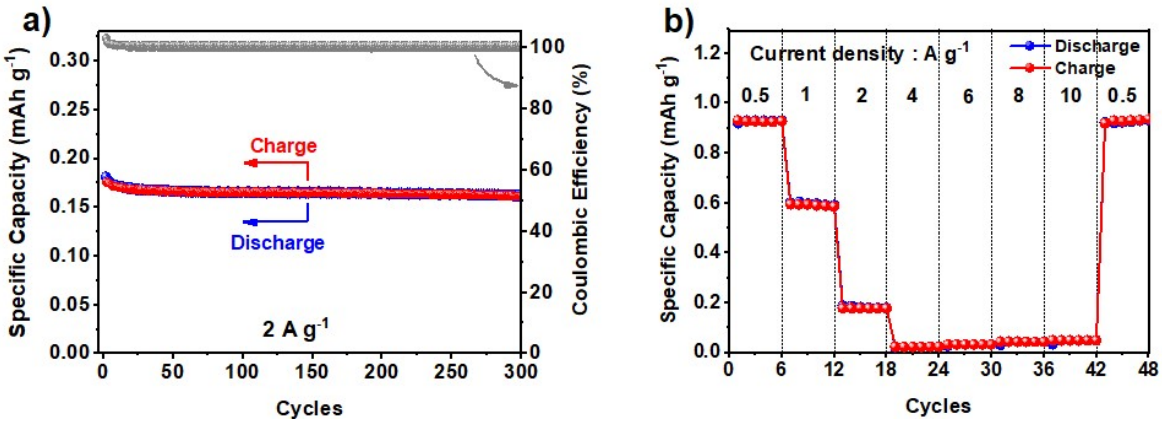

Fig. S2. Electrochemical performance of the current collector (carbon paper, Sigracet 25 BC). (a) Long-term cycling performance at a current density of 2 A g^{-1}. (b) Rate performance at different current densities.

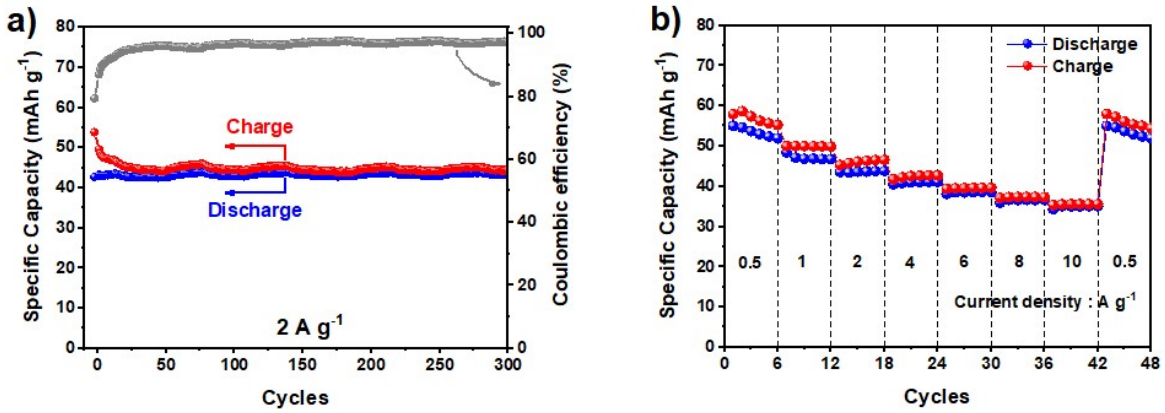

Fig. S3. Electrochemical performance of the super P electrode. The electrode was prepared by mixing 90% of conductive carbon (super P) with 10 % of polyvinylidene fluoride binder (PVDF) in N-methyl-2-pyrrolidinone (NMP) and then the mixture was painted on conductive carbon paper (Sigracet 25 BC, Fuell Cells Store, US). The 'wet' electrode was further dried for 4h in a 40°C oven after that at 80°C overnight under vacuum. (a) Long-term cycling performance at a current density of 2 A g^{-1}. (b) Rate performance at different current densities.

Theoretical capacity C_t

The theoretical capacity C_t (mAh g^{-1}) of PIT is calculated using the following Eq. (1) :

$$C_t = \frac{F}{3600(M_w/1000)} \qquad (1)$$

where F and M_w are the Faraday constant (96484 C mol^{-1}) and the molecular weight per active specie, respectively.[20]

In each PIT unit cell, 3 imide groups (6 x 1/2 =3), and 2 triazine rings (6 x 1/3 =2) are served as actives sites. The number of electrons (n) implicated in each unit cell of PIT is determined using the equation of 3 × 2 + 2 × 3= 12. The molecular weight of each unit cell could be calculated according to $M_{unit\ cell}$ = 3 × $M_{diimide}$ + 2 × $M_{triazine}$ = 3 × 214 + 2 × 81 = 804 g mol^{-1}. Thus the molecular weight per active specie (M_w = $M_{unit\ cell}$/12) is 67 g mol^{-1} and the theoretical capacity of PIT is found as 400 mA h g^{-1}.

References

1 T. Wang, R. Xue, H. Chen, P. Shi, X. Lei, Y. Wei, H. Guo and W. Yang, *New J. Chem.*, 2017, **41**, 14272–14278.
2 S. Chu, Y. Wang, Y. Guo, P. Zhou, H. Yu, L. Luo, F. Kong and Z. Zou, *J. Mater. Chem.*, 2012, **22**, 15519.
3 L. Lin, P. Ye, C. Cao, Q. Jin, G.-S. Xu, Y.-H. Shen and Y.-P. Yuan, *J. Mater. Chem. A*, 2015, **3**, 10205–10208.
4 J. Yang, S. Chu, Y. Guo, L. Luo, F. Kong, Y. Wang and Z. Zou, *Chem. Commun.*, 2012, **48**, 3533.
5 J.-Y. Li, X. Jiang, L. Lin, J.-J. Zhou, G.-S. Xu and Y.-P. Yuan, *J. Mol. Catal. Chem.*, 2015, **406**, 46–50.
6 Y. Luo, B. Li, L. Liang and B. Tan, *Chem. Commun.*, 2011, **47**, 7704.
7 H. Zhu, C. Wang, J. Zhou, M. Wan, Y. Wang, Z. Zou and M. Terrones, *J. Porous Mater.*, 2018, **25**, 1659–1668.
8 Y. Wang, Q. Gao, Q. You, G. Liao, H. Xia and D. Wang, *React. Funct. Polym.*, 2016, **103**, 9–16.
9 V. A. Kuehl, M. J. Wenzel, B. A. Parkinson, L. de Sousa Oliveira and J. O. Hoberg, *J. Mater. Chem. A*, 2021, **9**, 15301–15309.
10 Y. Zhang, M.-S. Zhang, Y. Zhang, X.-W. Chen and J.-H. Wang, *RSC Adv.*, 2016, **6**, 46002–46007.
11 P. Meng, J. Huang and X. Liu, *Appl. Surf. Sci.*, 2019, **465**, 125–135.
12 J. Zhou, Y. Wang, X. Hao, C. Ma, Y. Wang and Z. Zou, *J. Phys. Chem. C*, 2018, **122**, 1037–1043.
13 S. Chu, Y. Wang, C. Wang, J. Yang and Z. Zou, *Int. J. Hydrog. Energy*, 2013, **38**, 10768–10772.
14 Z. Luo, L. Liu, J. Ning, K. Lei, Y. Lu, F. Li, J. Chen, *Angew. Chem. Int. Ed.*, 2018, **57** ,9443–9446.
15 J. Zhao, T. Kang, Y. Chu, P. Chen, F. Jin, Y. Shen, L. Chen, *Nano Res.*, 2019, **12**, 1355–1360.
16 H. Wu, Q. Meng, Q. Yang, M. Zhang, K. Lu, Z. Wei, *Adv. Mater.*, 2015, **27**, 6504–6510.
17 C. Wua, M. Hua, X. Yana, G. Shanc, J. Liua, J. Yang, *Energy Stor. Mater.*, 2021, **36**, 347–354.
18 K. Li, Y. Wang, B. Gao, X. Lv, Z. Si, H.-G. Wang, *J. Colloid Interface Sci.*, 2021, **601**, 446–453.
19 G. Zhao, H. Li, Z. Gao, L. Xu, Z. Mei, S. Cai, T. Liu, X. Yang, H. Guo, X. Sun, *Adv. Funct. Mater.*, 2021, **31**, 2101019.
20 G. Zhao, H. Li, Z. Gao, L. Xu, Z. Mei, S. Cai, T. Liu, X. Yang, H. Guo and X. Sun, *Adv. Funct. Mater.*, 2021, **31**, 2101019.